

Diffusion Monte Carlo methods applied to Hamaker Constant evaluations

Kenta Hongo* and Ryo Maezono

School of Information Science, JAIST, Asahidai 1-1, Nomi, Ishikawa 923-1292, Japan

(Dated: April 23, 2019)

We applied diffusion Monte Carlo (DMC) methods to evaluate Hamaker constants of liquids for wettabilities, with practical size of a liquid molecule, Si_6H_{12} (cyclohexasilane). The evaluated constant would be justified in the sense that it lies within the expected dependence on molecular weights among similar kinds of molecules, though there is no reference experimental values available for this molecule. Comparing the DMC with vdW-DFT evaluations, we clarified that some of the vdW-DFT evaluations could not describe correct asymptotic decays and hence Hamaker constants even though they gave reasonable binding lengths and energies, and vice versa for the rest of vdW-DFTs. We also found the advantage of DMC for this practical purpose over CCSD(T) because of the large amount of BSSE/CBS corrections required for the latter under the limitation of basis set size applicable to the practical size of a liquid molecule, while the former is free from such limitations to the extent that only the nodal structure of the many-body wavefunction is fixed by a given basis set.

INTRODUCTION

Hamaker constants [1] dominate the wettability of solvents, which is one of the critical properties in industrial applications of Sol-Gel methods [2], including solution processes for semiconductor devices. [3, 4] Microscopic understanding of the wettability [5] relates the Hamaker constant with inter-molecular interactions, which can be, in principle, evaluated from ab-initio simulations. Once we could provide such database of inter-molecular interactions aided by recent ab-initio methods, we could predict, control, and design such solution processes including not only wettabilities but also suspensions and solvabilities by using empirical molecular dynamics simulations. [6–10] The framework of the ab-initio evaluation of inter-molecular interactions is straightforward, in principle. We can evaluate a binding curve by ground state energy calculations of coalescence geometries with varying the inter-molecular distance. Its long-range asymptotic behavior is fit by the power decay, extracting its coefficient corresponding Hamaker constants. Though we can find several such prototypical works [5] of the '*ab initio* assessment' applied to simple and highly symmetric molecules, we would immediately face to troubles when we try to apply the framework to practical solute molecules. This mainly arises from the following two factors: (1) As is well-known, accurate correlated methods such as CCSD(T) are required to get enough reliable estimations of inter-molecular interaction. [11, 12] Such methods are, in general, quite costly in the sense of the scalability on the system size N , *e.g.*, $\sim N^7$ for CCSD(T) [13]. Such severe scalabilities obstruct the applications to larger molecules being likely in the practical cases. (2) Most molecules of industrial interest are not highly symmetric, in general. In these cases, too many alignments of coalescence are possible due to the anisotropy of molecules, bewildering us how to model the coalescence with the confidence for capturing the nature

of the system.

For (1), DMC (diffusion Monte Carlo) method is quite promising with rapidly increasing capability for practical applications. [14, 15] This framework is regarded in principle as the most reliable that can achieve 'numerically exact solutions' in some cases, and there has been so far several applications to inter-molecular interactions, [16–25] to calibrate even over accurate molecular orbital methods such as CCSD(T). DMC scales at worst to $\sim N^3$, [26] making it possible to be applied further to larger molecules including molecular crystals. [22–25] In this study, we adopted DMC to get an advantage over the factor (1), aiming at constructing a scheme even valid for the challenge described as the factor (2) above. We applied the scheme to a cyclohexasilane molecule, Si_6H_{12} , which is used as an ink for 'printed electronics' technology to fabricate polycrystalline Si film transistors. [3, 27–29] The ink is painted and sintered on substrates to form amorphous Si for the fabrication, avoiding expensive vacuum environments in the conventional semiconductor processes. The ink printing process is hence attracting recent interests for realizing more@saving and low environmental impact technology. [3, 4, 27–36] Controlling the wettability of these inks is of rather general interests because the technology is about to be applied further to fabricate oxide semiconductor devices [32–35] and carbon nanotube film semiconductor devices, [36] by using variety of inks not only of Si-based ones. For going beyond conventional/experimental preparations of inks, several simulations have been made to analyze the wettability of droplets on ink-jet processes dynamically using molecular dynamics [6–8] or empirical models [9, 10]. The predictability of these simulations is critically depending on the force fields that are currently prepared by empirical parameterizations of Lennard-Jones type potentials. The ab-initio assessment for these parameterizations is obviously recognized as an important breakthrough in getting more universal applicability. However, commonly

available framework, DFT (density functional theory), is known to fail to describe inter-molecular interactions universally, and the DFT performance strongly depends on exchange-correlation (XC) functionals adopted. [12] In the present case, the interaction of this system, cyclohexasilane, is of non- π stacking nature, known as an *aliphatic-aliphatic* one [37] between the σ bonds at the HOMO (highest-occupied molecular orbital) levels of the monomers. Unlike *aromatic-aromatic* interactions of *e.g.* benzene dimer, there has been not enough preceding investigations on *aliphatic-aliphatic* interactions and hence no established scheme of how to treat the anisotropy of molecules in the evaluation of binding curves even for moderately tractable size and symmetry of the target molecules.

In this study, we have established a scheme to give ab-initio estimations of Hamaker constants using DMC method. For the anisotropy issue described above as (2), we took three typical configurations of coalescence and considered an averaging and weighting scheme over them. We got fairly reasonable coincidence between estimated and experimental specific weights, densities, and binding energies. For further calibration, we also made a comparison of numerical results between DMC and CCSD(T), getting good agreements in both fittings for the long-range exponents ($\sim 1/R^6$) and Lennard-Jones potential parameters. The estimated Hamaker constants are confirmed to be within the reasonable range, which is estimated separately by another theoretical approach to the wettability, the Lifshitz theory, applied to the same kinds of cyclosilane molecules.

The paper is organized as follows: In the next section, we provide computational methods in detail. Results are summarized in the following section. Discussions are given in the separate section, where we estimate densities and Hamaker constants from evaluated binding curves, and then compared them with experimental values. Summaries of the paper are given as Concluding Remarks at the end of main text. For detailed correction schemes, such as BSSE (basis set superposition error), CBS (complete basis set) schemes as well as time-step error in DMC are given in Supporting Information.

COMPUTATIONAL METHODS

Our aim is to establish an *ab initio* assessment scheme of evaluating Hamaker constants from long-range behavior of dimer binding curves for cyclohexasilane (CHS). Similar to cyclohexane, CHS has several types of conformations such as chair and boat ones [38, 39]. Since the chair conformer is known to be most stable, we consider only a pair of the chair conformers as the dimer, but three types of dimer coalescences, *i.e.*, parallel-wise or face-to-face (Type-A), T-shaped (Type-B), and in-line-

wise (Type-C), as shown in Fig. 1. Inferring from the cyclohexane case [37], Type-A can be expected to be most stable at its equilibrium geometry, but the other two possibilities, Type-B and -C, are also taken into account, because our concern is their long-range as well as equilibrium behaviors. In order to evaluate its binding curves, each monomer structure in a dimer coalescence is fixed at each binding distance, where the distance between the monomers is defined as that between the centers of gravity of the monomers. This is justified to some extent because we focus on the behavior at longer inter-molecular distances, where the monomer structure would be almost the same as that of an isolated monomer. The constituent monomer geometry is optimized at the B3LYP/6-311G level of theory using Gaussian09. [40]

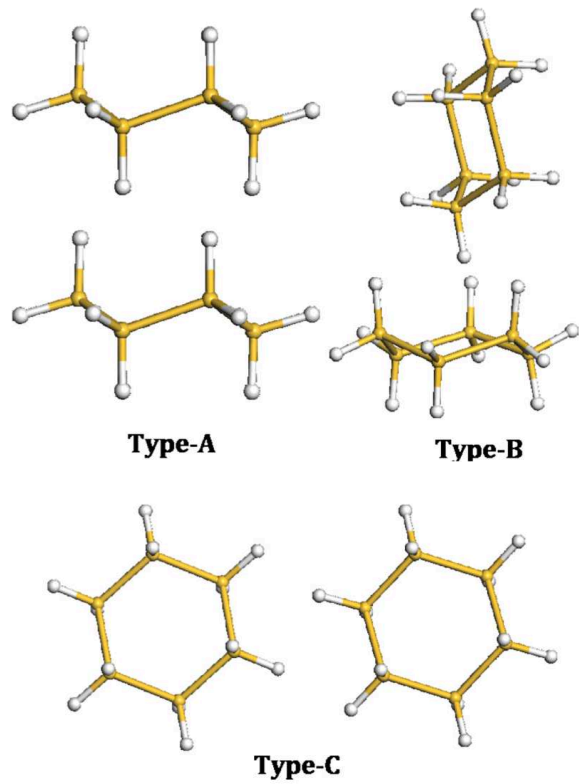


FIG. 1. Typical configurations of the dimer coalescence considered in this work, Parallel or 'face to face' (Type-A), T-shaped (Type-B), and in-plane-wise (Type-C).

The binding curves are evaluated by DMC, compared with CCSD(T), MP2, and several DFT calculations with various XC functionals. As a common choice, the fixed-node approximation [14, 15] was made to the DMC simulations (FNDDMC), taking Slater-Jastrow wavefunctions as the guiding functions. The Slater determinants are composed of Kohn-Sham (KS) orbitals obtained using Gaussian09 [40] with Burkatzki-Filippi-Dolg (BFD) pseudo potentials (PP) [41] and its accompanying VTZ

Gaussian basis sets. The BFD-PPs have been proved to give enough practical accuracies not only in DMC but also DFT on the applications such as a DNA stacking problem. [22] Only for Type-A, we examined LDA, PBE, and B3LYP functionals to see how the choice of the XC functionals affects the trial nodal structures in FNDMC. As we demonstrate later, all the three functions give almost the same binding energy and equilibrium distances, but B3LYP is found to give the best nodal surface in the sense of the variational principle. Hence we concentrated only on B3LYP orbitals for DMC for Type-B and -C. Our Jastrow functions [42, 43] were those implemented in CASINO [14], consisting of one-, two-, and three-body contributions, denoted as χ -, u -, and F -terms, respectively. The χ -, u -, and F -terms include 16, 16, and 32 adjustable parameters, respectively. They were optimized by the variance minimization scheme [44, 45]. The electron-electron cusp condition [46] was imposed only on the u -term during the optimization procedure. For DMC statistical accumulations, we set the target population (the number of random walkers) to be 1,024 configurations in average and the time step to be $\delta t = 0.02$ in atomic unit. The time step bias [47] arising from this choice is discussed in Supporting Information. We took averages over 1.7×10^5 accumulation steps after the equilibration of 10^3 steps. We also used T -move scheme [48] for the locality approximation to the evaluation of PPs [49, 50] in DMC.

We benchmarked various DFT-SCF calculations for a comparison with FNDMC. Our choice of XC functionals in DFT includes those recently designed for intermolecular interactions, B3LYP+GD2 [51]/GD3, [52] M06-2X, [53] and B97-D, [51] as well as LDA [54], PBE [55], B3LYP [56–58]. For a systematic comparison, we consistently used the same basis sets as FNDMC, VTZ basis sets provided in BFD-PP library [41]. For correlated methods (MP2 and CCSD(T)), however, the VTZ is too large to be accommodated in tractable memory capacities (512GB shared by 64 parallel cores in SGI Altix UV1000). To correct biases due to basis sets choices, we used two different kinds of Complete Basis Set (CBS) methods [59, 60], and the Counterpoise method for basis set superposition error (BSSE). [13, 61–63] Detailed discussions about these corrections are given in Supporting Information. All the DFT-SCF and correlated calculations were performed using Gaussian09. [40]

RESULTS

Binding curve

Fig. 2 highlights typical binding curves evaluated by various methods, though only for Type-A (for the other types, see Supporting Information). All the SCF curves

were corrected by the BSSE scheme [13, 61–63] (see Supporting Information). The present study takes CCSD(T) as a standard reference to calibrate the performance of the SCF approaches. We can find the DFT predictions scattering around CCSD(T). Except LDA, conventional functionals such as PBE and B3LYP fail to capture the binding itself. The LDA overbinding has been frequently reported for several inter-molecular bindings. [22–25, 64, 65] This can be regarded as spurious due to improper self interactions: Exchange repulsion is not fully reproduced in LDA because of the lack of the exact cancellation of self interaction, and hence spurious 'chemical' bindings are formed due to the weakened repulsions, rather than true inter-molecular bindings. The exchange repulsion weakened in LDA gets recovered when changing XC into GGA and further into B3LYP, which may explain the rising-up of the curves pushing the minimum toward distant region. As discussed later in Discussion section, we tried two possible estimations for Hamaker constants, A_6 and A_{LJ} , as shown in Table II. A significant difference in LDA between A_6 and A_{LJ} implies poor reliability on its long-range behavior description.

The XC functionals for inter-molecular interactions, M06-2X, B97-D and B3LYP-GD(2,3), on the other hand, well reproduce the bindings at their equilibrium lengths, as seen in Fig. 2. We see, however, that M06-2X and B3LYP-GD2 give rise to less reliable asymptotic behaviors at long-range region, where they decay much faster than CCSD(T) or the other XC functionals for intermolecular interactions. As for M06-2X, its functional form based on hybrid meta-GGA does not explicitly contain dispersion interactions by its construction, and its parameterizations of the XC functionals are adjusted so as to reproduce a number of molecular bindings *around* their equilibrium geometries, giving rise to the unreliable long-range behavior. B97-D and B3LYP-GD2 are classified into the DFT-D2 family including 'atom-pairwise' second-order perturbative dispersion corrections (two-body term). [51] Both B97-D and B3LYP-GD2 give poor estimates of binding energies and lengths, but the former behaves better than the latter at long-range region, being appropriate for the estimation of Hamaker constants. This implies long-range behaviors also depend on original functionals, and atom-pairwise dispersion corrections do not necessarily lead to a correct description of 'molecule-pairwise' dispersion interactions, as in the B3LYP-GD2 case. It has been reported that DFT-D3 including atom-pairwise third-order perturbative dispersion corrections (three-body term) can remedy this kind of discrepancy in long-range as well as equilibrium behaviors at the DFT-D2 level of theory [52]. It is notable that the present B3LYP-GD3 binding curve is well improved in its long-ranged behavior to reproduce correct decaying exponent. For the present CHS case, its correct molecule-pairwise dispersion behavior at long-range region requires both

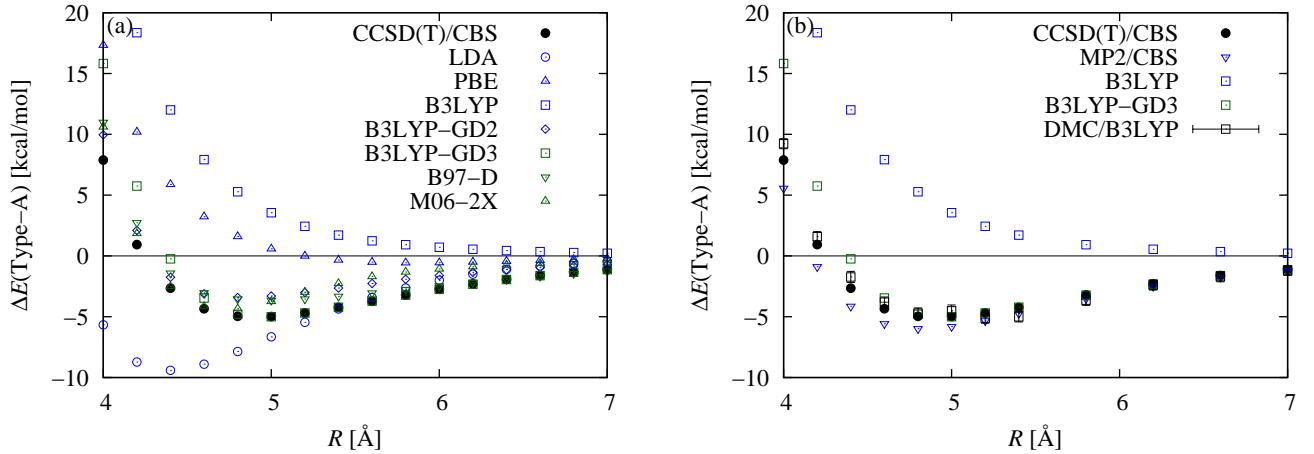


FIG. 2. Binding curves of Type-A (parallel) dimer coalescence evaluated by (a) DFT methods (LDA, PBE, B3LYP, B3LYP-GD2/GD3, B97-D, M06-2X) and (b) correlation methods (MP2, CCSD(T) and DMC/B3LYP) compared with selected DFTs. All the curves (except DMC) are corrected by BSSE and CBS (see Supporting Information for more details).

the second- and third-order perturbative dispersion corrections. Looking at the short-range region, on the other hand, we find that B97-D and M06-2X gives a better description than B3LYP-GD3, getting closer to the DMC and CCSD(T) estimations. This suggests that B3LYP-GD3 includes too large Hartree-Fock exchange effects to be adequately canceled out by correlation effects. The above results can be summarized in Table I.

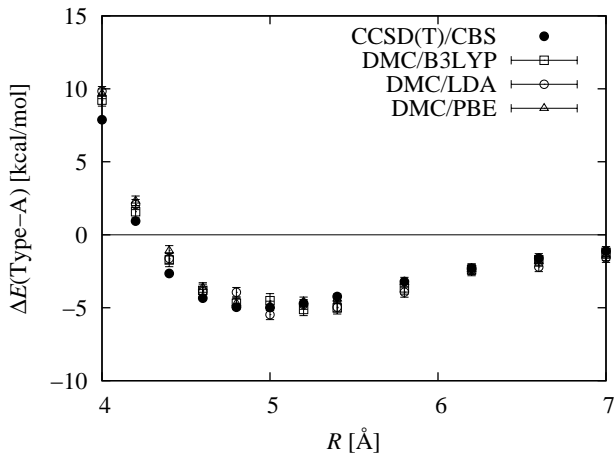


FIG. 3. Comparison of DMC binding curves obtained by different nodal surfaces generated by LDA, PBE, and B3LYP (e.g., 'DMC/PBE' stands for DMC by B3LYP nodal surface). CCSD(T) result is also shown for comparison, which is corrected by BSSE and CBS (see Supporting Information for more details).

Our FNDMC and MP2 results are shown in Fig. 2 (b), compared with CCSD(T) and typical SCF (B3LYP).

As is well known, MP2 overbinds with deeper (shorter) binding energy (distance). [66] It may not be surprising to get the coincidence of asymptotic behaviors between MP2 and CCSD(T), because the present CCSD(T) is corrected by the CBS scheme taken from MP2 [60] (see Supporting Information). Three DMC curves were obtained starting from guiding functions generated by LDA, PBE, and B3LYP, respectively. They converged almost to the same binding curve, even starting from either B3LYP (worst in reproducing binding in SCF level) or LDA (too deep spurious overbinding in SCF). Similar insensitivity to the choice of guiding functions has been also reported for a DNA stacking case, [22] implying that these DMC predictions are not seriously affected by the fixed-node approximation. Based on the variational principle with respect to nodal surfaces in FNDMC [48–50], we henceforth concentrate on the B3LYP guiding function only, because it gives the lowest total energy though the energy differences among the three binding curves are quite small.

Binding energies (ΔE), equilibrium lengths (R_{eq}), and estimated Hamaker constants (A) are summarized in Table II. The present DMC is found to give almost the same results as CCSD(T). Their estimated binding energies are comparable with the typical value of non- π stacking energies ~ -5 kcal/mol. [37] Compared with π -stacking energies, it is about twice larger, which would be consistent with the higher boiling temperature of CHS than that of its structural isomers with the same molecular weights but without hydrogen bindings. [67] A remarkable difference between CCSD(T) and FNDMC is the binding energy at short range, $\Delta E(4.0)$ by ~ 1 kcal/mol. The difference would be partly attributed to the dynamical correlation effect, which becomes more important at

	Binding Energy	Short-range	Long-range@
B3LYP-GD2	NG	NG	NG
B3LYP-GD3	G	NG	G
B97-D	NG	NG	G
M06-2X	G	NG	NG
MP2	NG	NG	G

TABLE I. Summary of the abilities in describing each binding region by each method. NG/G stands for 'No Good'/'Good', respectively.

shorter binding length as well as exchange repulsions. Even under the fixed-node approximation, the dynamical correlation is expected to be well described, [14–25] and hence the present DMC curve is regarded as the best description of the binding of CHS.

DISCUSSION

Long-range behavior: Hamakar constant

Asymptotic exponents can be extracted from log-plots of long-range behaviors, as shown in Fig. 4. The best fits of the exponents in DMC [CCSD(T)] give -5.6 ± 5.8 [-5.9], -4.2 ± 5.9 [-7.3], and -7.2 ± 7.2 [-8.7] for Type-A, B, and C, respectively. Supported by CCSD(T) estimations, we can somehow identify that Type-A dominates the wettability with the longest-ranged exponent being almost close to the $\sim C_6/R^6$ dependence. For Type-A, we can then identify the C_6 constant from the fitting with exponent fixed to 6.0. The experimental density, $\rho = 0.323 \times 10^{28} [1/m^3]$ at 298.15K, then gives an estimation of the Hamaker constant, $A = \pi \rho^2 C_6$, as 99 ± 25 zJ [95 zJ] by DMC [CCSD(T)]. We notice that the DMC estimation here is less convincing because of the too large errorbar. This is actually a sort of inevitable consequence of log-plots for long-range exponents: [68] For a fixed magnitude of statistical errors over the range of distance R , any decreasing dependence on a log-plot gives inevitably enlarged errorbars as R increases (the resolution of the vertical axis gets enlarged downward). If we aimed to reduce the errorbar by one more digit, 100 times more statistical accumulation is required. This corresponds to 2.2×10^6 core-hours (half a year CPU time on 512 cores parallel, provided that we can keep on using it without any queue), and hence is impractical.

To avoid using such larger errorbars, we tried another fitting scheme based on 6-12 Lenard-Jones potential,

$$U(R) = -\frac{C_6}{R^6} + \frac{C_{12}}{R^{12}}, \quad (1)$$

as shown in Fig. 5. The fitting to DMC [CCSD(T)] data gives the estimations of C_6 , and then the Hamaker constant as, $A_{\text{LJ}} = 104 \pm 4$ zJ [99 zJ], keeping the consistency with those estimated by log-plots with much improved statistical noise.

Since there is no reference values of A to be compared directly to the present estimation for CHS, we tried a justification via side-way manner as below: For several systems with similar kinds of molecules, two different estimations of Hamaker constants, A_{Hamaker} and A_{Lifshitz} , are available, as shown in Table III. While A_{Hamaker} is a rather direct estimation from C_6 , A_{Lifshitz} is a sort of model estimation using Lifshitz theory. [69] Under an approximation using Parsegian-Ninham representation [70] for dielectric function, A_{Lifshitz} can be evaluated from dielectric constants, refractive constants, and IR/UV (infra-red/ultra violet) absorption frequencies, which are available from experiments. [71] We can then estimate A_{Lifshitz} over several cycloalkanes, $C_n H_{2n}$ ($n = 5, 6, 8$), as shown in Table III. Though there is no *a priori* reasons found, we can see trends such that: i) A_{Lifshitz} almost linearly depends on n , and ii) the ratio, $A_{\text{Hamaker}}/A_{\text{Lifshitz}}$, is almost always around $1.3 \sim 1.5$. From the trend (i), we can estimate A_{Lifshitz} for CHS being ~ 73 zJ, and then the resultant ratio, $A_{\text{Hamaker}}/A_{\text{Lifshitz}} = 1.37$, lies within the expected range from (ii).

The reason why Hamaker's naive evaluation generally overestimates A values compared with the Lifshitz theory may be explained as follows: A_{Hamaker} is evaluated only from the longest-ranged exponent with a selected coalescence configuration, Type-A in the present case. Other configurations with shorter-ranged exponents should be included in liquids by some fractions, and hence effectively weaken the binding strength estimated under such an assumption with 100% constitution of Type-A coalescence. Such an effect would be represented as 'effectively reduced' Hamaker constants being close to A_{Lifshitz} . Hence, the values, $A_{\text{Hamaker}}/A_{\text{Lifshitz}}$, could be sorted out by a factor dominating the fraction, $\exp(-\Delta E/kT)$, where ΔE denotes a typical energy difference between the coalescence configurations with the longest- and the shortest-ranging exponents.

Equilibrium behavior: Density

We can directly estimate the binding energy, ΔE , and the equilibrium binding length, R_{eq} , by fitting the data

	LDA	M06-2X	B3LYP-GD3	MP2	CCSD(T)	DMC
$\Delta E(4.0)$	-5.67	10.60	15.82	5.56	7.89	9.2(4)
$\Delta E(R_{\text{eq}})$	-9.39	-3.75	-5.06	-6.36	-5.34	-5.3(2)
R_{eq}	4.34	4.67	4.93	4.70	4.83	4.89(2)
A_6	48	36	96	104	95	99(25)
A_{LJ}	90	56	105	99	97	104(4)

TABLE II. Estimated binding energies, ΔE [kcal/mol], equilibrium binding lengths, R_{eq} [Å], and two different estimations of Hamaker constant, $A_{6/\text{LJ}}$ [zJ] (see text for more details about the definitions). Statistical errors in the DMC values are given in parenthesis. PBE and B3LYP are left out because they give repulsive binding curves at long range and hence their Hamaker constants cannot be evaluated.

	H ₂ O	C ₆ H ₆	CCl ₄	CH ₃ OH	C ₅ H ₁₀	C ₆ H ₁₂	C ₈ H ₁₆	CPS	CHS
A_{Hamaker}	48 ^a	74 ^a	74 ^a	46 ^a	-	-	-	-	~ 100
A_{Lifshitz}	37 ^a	50 ^a	55 ^a	36 ^a	49 ^b	53 ^b	58 ^b	68 ^b	~ 73
$A_{\text{Hamaker}}/A_{\text{Lifshitz}}$	1.29	1.49	1.34	1.29	-	-	-	-	~ 1.37

TABLE III. Two different estimations of Hamaker constants, A_{Hamaker} and A_{Lifshitz} , given in the unit of [zJ], evaluated at $T = 298.15$ K.

using an equivalent form of Eq. (1),

$$U(R) = \Delta E \left[2 \left(\frac{R_{\text{eq}}}{R} \right)^6 - \left(\frac{R_{\text{eq}}}{R} \right)^{12} \right], \quad (2)$$

as summarized in Table IV. Note that we can also estimate ΔE and R_{eq} 'after' the fitting (C_6, C_{12}) first by Eq. (1), but this is not a good idea for DMC because the error propagation for statistical noises during the further transformation to ΔE and R_{eq} loses the accuracy of estimates. Fitting curves well describe the dependence around equilibrium lengths, as shown in Fig. 5. For Type-B and C with shorter-ranged exponents, it is not rigorously justified to use LJ potential because it supposes $1/R^6$ asymptotic behavior. We use it, however, under such a limited reason just to get possible estimates of ΔE and R_{eq} even for Type-B and C, as summarized in Table IV.

Though there is no reference available for a direct comparison with the estimated binding lengths, we can derive a possible value from experimental values of the molecular weight (180.61 g/mol) and density (0.97 g/cm³ at $T = 298.15$ K). The resultant value for the mean intermolecular separation is 6.8 Å, which fairly reasonably drops within the binding lengths of Type-A to C. We then come to consider how to put the weight on each binding length to get a reasonable average over the configurations so as to get the average closer to the experimental mean value. One possibility would be the thermal averaging, \bar{R} , by the factor $p \sim \exp(-\Delta E/kT)$, also summarized in Table IV at $T = 298.15$ K. In this weighting, however, the Boltzmann factor of Type-A is dominant to give, $\bar{R} \sim 4.9$ Å. This is quite shorter than the experimental estimation of 6.8 Å. The discrepancy should, as a matter of course, be attributed to such factors that are not taken into account in the present estimation. The

intra-molecular structural relaxation brought by the coalescence is one of such factors but this seems not accounting for it: the relaxation will bring energy gains at shorter binding lengths and hence make the present prediction corrected shorter, further away from the experimental mean. As another factor, we notice that we took into account only two-body coalescences to argue the mean separation. When we consider further four-body clusterings possibly occurring in realistic liquids, we notice that the mean separation seems to be dominated rather by the longest binding length among the possible coalescence: The mean value can roughly be estimated by the 'diagonal lengths' of four-body trapezoids, as shown in Fig. 6. Taking the center of gravity of each molecule as the vertices of trapezoids, the 'diagonal lengths' can be defined as the square root of the area of a trapezoid, which is dominated rather by the longest distant binding pair. Estimating the possibility weight for each trapezoid as the Boltzmann weight with the sum of the binding pair energies, ΔE , then the thermal averaging over the 'diagonal lengths' gives an improved estimate, getting closer to the experimental estimation, as shown in Table V.

Practicality compared with CCSD(T)

Fig. 7 shows the comparison between DMC and CCSD(T) with and without basis set corrections. Even though CCSD(T) is known as the 'Gold standard' among *ab-initio* predictions, the practical use of CCSD(T) requires very careful handling of corrections, as described in Supporting Information, to get enough reliable predictions. [72] The correction itself is also under quite a limited approximation [59, 60] (see Eq. (1) in Supporting Information). These practical limitations are, in contrast, not the case in DMC because it is free from the

	B3LYP-GD3	MP2	CCSD(T)	DMC
$p(A)/R_{\text{eq}}$	0.971/4.9	0.976/4.7	0.968/4.8	0.987(82)/4.83(2)
$p(B)/R_{\text{eq}}$	0.026/6.6	0.023/6.1	0.030/6.2	0.010(24)/6.37(6)
$p(C)/R_{\text{eq}}$	0.003/8.8	0.002/8.4	0.003/8.6	0.003(14)/8.7(1)
\bar{R}_{dim}	5.0	4.7	4.9	4.9(1)

TABLE IV. Comparisons of the equilibrium stabilities among three coalescence configurations in Fig. 1, in terms of the thermal probability weight, $p \sim \exp(-\Delta E/kT)$. Equilibrium binding lengths, R_{eq} [Å], are also shown. \bar{R}_{dim} [Å] is the thermal averaged binding lengths at $T = 298.15$ K for each method.

	B3LYP-GD3	MP2	CCSD(T)	DMC
$p(\alpha)/R_{\text{diag}}$	0.343/6.6	0.293/6.3	0.327/6.4	0.48(27)/6.5
$p(\beta)/R_{\text{diag}}$	0.243/6.7	0.248/6.3	0.245/6.5	0.21(7)/6.6
$p(\gamma)/R_{\text{diag}}$	0.243/6.6	0.248/6.1	0.245/6.3	0.21(7)/6.4
$p(\delta)/R_{\text{diag}}$	0.172/6.6	0.210/6.1	0.183/6.2	0.09(19)/6.4
\bar{R}_{tetra}	6.6	6.2	6.4	6.5(2)

TABLE V. Comparisons of the equilibrium stabilities among four clustering configurations in Fig. 6, in terms of the thermal probability weight, $p \sim \exp(-\Delta E/kT)$. R_{diag} [Å] stands for the diagonal length for each tetramer, and \bar{R}_{tetra} [Å] is the thermal averaged diagonal length at $T = 298.15$ K.

basis set choice to the extent that only the nodal structure of the many-body wavefunction is fixed by the given basis set. DMC therefore possesses the advantage for the purpose to evaluate Hamaker constants over CCSD(T) with less sensitivity to basis sets for practically larger systems.

CONCLUDING REMARKS

We provide a framework using DMC to evaluate Hamaker constants for practical isotropic molecules, and applied it to a cyclohexasilane molecule used as an ink for printed electronics. The framework takes into account two important factors for practical applications, namely the weak inter-molecular interactions dominated by electron correlations, and non-unique coalescing direction between anisotropic molecules. Our DMC results coincides fairly well with other correlation methods such as CCSD(T), MP2, and several DFT with exchange-correlation functionals for inter-molecular interactions, like B3LYP-GD3. The evaluated binding curve can reasonably explain the experimental density of the liquid solution, as well as the trend of boiling temperatures. We find out that the parallel-wise coalescence of molecules gives the longest distant exponent for the interaction, being around 6.0, which can then be well fitted by the Lenard-Jones potential. The fitting gives an estimation of Hamaker constant being 104 ± 4 zJ, with practically enough small statistical error. Though there is no experimental data available for a direct comparison, the present estimation is well supported from the trend of both Hamaker constants for similar kinds of molecules and of systematic difference between the predictions by the Lifshitz theory and by the asymptotic exponent es-

timations. In the latter trend, we found the ratio of the prediction from the asymptotic exponent to that from the Lifshitz theory being always around 1.3 for several molecules.

ASSOCIATED CONTENT

The BSSE and CBS corrections to the SCF and correlated methods and the time-step bias in DMC are discussed in more detail at Supporting Information.

ACKNOWLEDGMENTS

The authors thank Mr. M. Imamura for his intensive preliminary calculations. K.H. is grateful for financial support from a KAKENHI grant (15K21023). The authors also acknowledge the support by the Computational Materials Science Initiative (CMSI/Japan) for the computational resources, Project Nos. hp120086, hp140150, hp150014 at K-computer, and SR16000 (Center for Computational Materials Science of the Institute for Materials Research, Tohoku University/Japan). R.M. is grateful for financial support from MEXT-KAKENHI grants 26287063, 25600156, 22104011 and that from the Asahi glass Foundation. The computation in this work has been partially performed using the facilities of the Center for Information Science in JAIST.

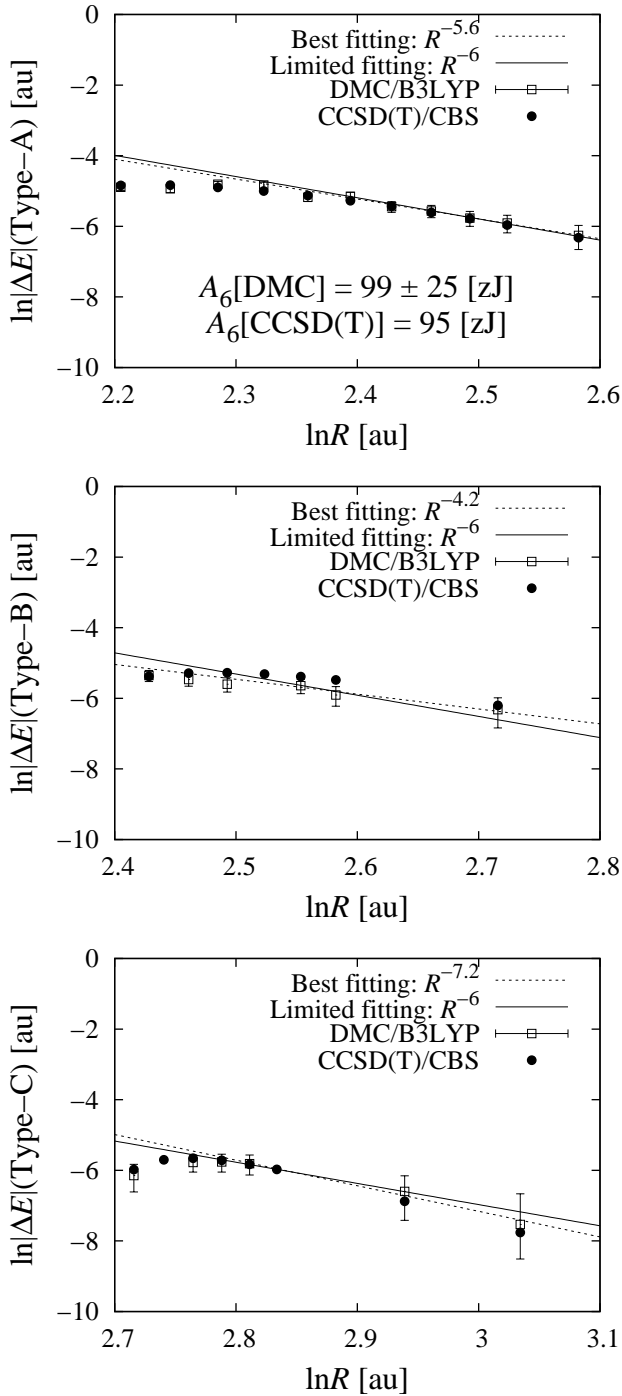


FIG. 4. Asymptotic behaviors of binding curves evaluated by DMC and CCSD(T), as given in logarithmic plots fitted by two different lines, 'Best' and 'Limited'. In the former fitting, the exponent is fitted to get the best fitting while in the latter it is fixed to be assumed R^{-6} behavior.

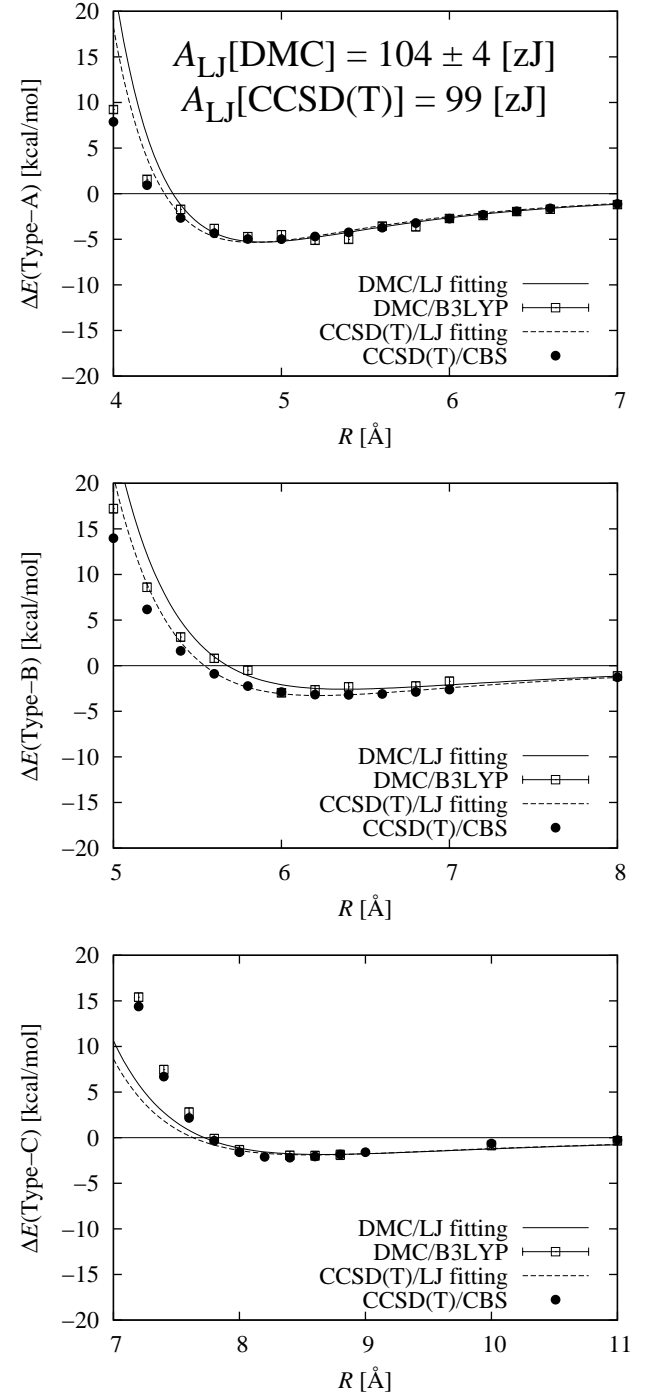


FIG. 5. Lennard-Jones fitting of DMC binding curve for each coalescence (Type-A to C) compared with CCSD(T). For Type-B and C, the fitting has a limited meaning because their asymptotic behavior are found not being R^{-6} (see text for details).

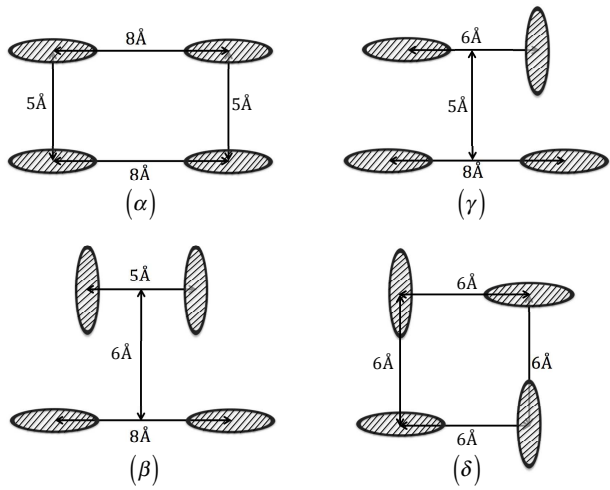


FIG. 6. Possible four-body clusterings formed from the two-body coalescences Fig. 1. Hatched regions stand for the surfaces surrounded by the ring of cyclohexasilane molecule.

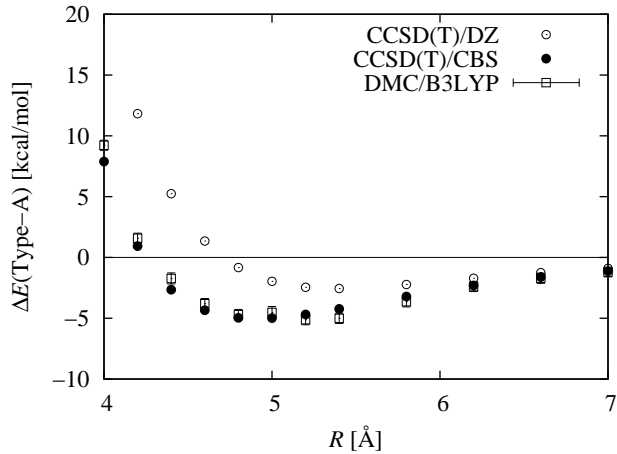


FIG. 7. Comparison of binding curves between FNDMC and BSSE-corrected CCSD(T) with the CBS/DZ basis set. 'CCSD(T)/DZ[CBS]' stands for the raw value without any corrections by DZ basis sets [CBS limit], while 'BSSE-CCSD(T)/DZ[CBS]' means that with BSSE corrections.

364 (2011).

- [5] J. N. Israelachvili, *Intermolecular and Surface Forces (Third Edition)*, third edition ed., tagkey2011iii (Academic Press, San Diego, 2011).
- [6] S. Maruyama, T. Kurashige, S. Matsumoto, Y. Yamaguchi, and T. Kimura, *Microscale Thermophysical Engineering* **2**, 49 (1998), <http://dx.doi.org/10.1080/108939598200105>.
- [7] G. Taura and M. Matsumoto, *Journal of Fluid Science and Technology* **5**, 207 (2010).
- [8] Y. Nakamura, A. Carlson, G. Amberg, and J. Shiomi, *Phys. Rev. E* **88**, 033010 (2013).
- [9] H. Matsui, Y. Noda, and T. Hasegawa, *Langmuir* **28**, 15450 (2012), <http://dx.doi.org/10.1021/la303717n>.
- [10] Y. Noda, H. Matsui, H. Minemawari, T. Yamada, and T. Hasegawa, *Journal of Applied Physics* **114**, 044905 (2013).
- [11] P. Hobza and K. Muller-Dethlefs, *Non-Covalent Interactions*, RSC Theoretical and Computational Chemistry Series (The Royal Society of Chemistry, 2009) pp. P001–P226.
- [12] A. J. Cohen, P. Mori-Sánchez, and W. Yang, *Chemical Reviews* **112**, 289 (2012), <http://dx.doi.org/10.1021/cr200107z>.
- [13] T. Helgaker, P. Jørgensen, and P. Olsen, *Molecular Electronic-Structure Theory* (Wiley, Chichester, U.K., 2000).
- [14] R. J. Needs, M. D. Towler, N. D. Drummond, and P. L. Ríos, *Journal of Physics: Condensed Matter* **22**, 023201 (2010).
- [15] B. M. Austin, D. Y. Zubarev, and W. A. Lester, *Chemical Reviews* **112**, 263 (2012), <http://pubs.acs.org/doi/pdf/10.1021/cr2001564>.
- [16] J. C. Grossman, *The Journal of Chemical Physics* **117**, 1434 (2002).
- [17] M. Korth, A. Luchow, and S. Grimme, *The Journal of Physical Chemistry A* **112**, 2104 (2008), <http://pubs.acs.org/doi/pdf/10.1021/jp077592t>.
- [18] L. Horváthová, M. Dubecký, L. Mitas, and I. Štich, *Journal of Chemical Theory and Computation* **9**, 390 (2013), <http://pubs.acs.org/doi/pdf/10.1021/ct300887t>.
- [19] L. Horváthová, R. Derian, L. Mitas, and I. Štich, *Phys. Rev. B* **90**, 115414 (2014).
- [20] M. Dubecký, P. Jurečka, R. Derian, P. Hobza, M. Otyepka, and L. Mitas, *Journal of Chemical Theory and Computation* **9**, 4287 (2013), <http://pubs.acs.org/doi/pdf/10.1021/ct4006739>.
- [21] M. Dubecký, R. Derian, P. Jurečka, L. Mitas, P. Hobza, and M. Otyepka, *Phys. Chem. Chem. Phys.* **16**, 20915 (2014).
- [22] K. Hongo, N. T. Cuong, and R. Maezono, *Journal of Chemical Theory and Computation* **9**, 1081 (2013), <http://pubs.acs.org/doi/pdf/10.1021/ct301065f>.
- [23] K. Hongo, M. A. Watson, R. S. Sánchez-Carrera, T. Iitaka, and A. Aspuru-Guzik, *The Journal of Physical Chemistry Letters* **1**, 1789 (2010), <http://pubs.acs.org/doi/pdf/10.1021/jz100418p>.
- [24] M. A. Watson, K. Hongo, T. Iitaka, and A. Aspuru-Guzik, "A benchmark quantum monte carlo study of molecular crystal polymorphism: A challenging case for density-functional theory," in *Advances in Quantum Monte Carlo*, Chap. 10, pp. 101–117, <http://pubs.acs.org/doi/pdf/10.1021/bk-2012-1094.ch009>.

* kenta_hongo@mac.com

- [1] H. Hamaker, *Physica* **4**, 1058 (1956).
- [2] D. Levy and M. Zayat, eds., *The Sol-Gel Handbook: Synthesis, Characterization and Applications, 3-Volume Set* (Wiley, 2015).
- [3] T. Shimoda, Y. Matsuki, M. Furusawa, T. Aoki, I. Yudasaka, H. Tanaka, H. Iwasawa, D. Wang, M. Miyasaka, and Y. Takeuchi, *Nature* **440**, 783 (2006).
- [4] H. Minemawari, H. Matsui, J. Tsutsumi, S. Haas, R. Chiba, R. Kumai, and T. Hasegawa, *Nature* **475**,

[25] K. Hongo, M. A. Watson, T. Iitaka, A. Aspuru-Guzik, and R. Maezono, *Journal of Chemical Theory and Computation* **11**, 907 (2015), pMID: 26579744, <http://dx.doi.org/10.1021/ct500401p>.

[26] A. Aspuru-Guzik, R. Salomón-Ferrer, B. Austin, and W. A. Lester, *Journal of Computational Chemistry* **26**, 708 (2005).

[27] T. Masuda, N. Sotani, H. Hamada, Y. Matsuki, and T. Shimoda, *Applied Physics Letters* **100**, 253908 (2012).

[28] J. Zhang, M. Trifunovic, M. van der Zwan, H. Takagishi, R. Kawajiri, T. Shimoda, C. I. M. Beenakker, and R. Ishihara, *Applied Physics Letters* **102**, 243502 (2013).

[29] Z. Shen, T. Masuda, H. Takagishi, K. Ohdaira, and T. Shimoda, *Chem. Commun.* **51**, 4417 (2015).

[30] Z. Shen, J. Li, Y. Matsuki, and T. Shimoda, *Chem. Commun.* **47**, 9992 (2011).

[31] Z. Shen, Y. Matsuki, and T. Shimoda, *Journal of the American Chemical Society* **134**, 8034 (2012), <http://dx.doi.org/10.1021/ja301956s>.

[32] J. Li, T. Kaneda, E. Tokumitsu, M. Koyano, T. Mitani, and T. Shimoda, *Applied Physics Letters* **101**, 052102 (2012).

[33] J. Li, E. Tokumitsu, M. Koyano, T. Mitani, and T. Shimoda, *Applied Physics Letters* **101**, 132104 (2012).

[34] K. Umeda, T. Miyasako, A. Sugiyama, A. Tanaka, M. Suzuki, E. Tokumitsu, and T. Shimoda, *Journal of Applied Physics* **113**, 184509 (2013).

[35] S. Inoue, T. Ariga, S. Matsumoto, M. Onoue, T. Miyasako, E. Tokumitsu, N. Chinone, Y. Cho, and T. Shimoda, *Journal of Applied Physics* **116**, 154103 (2014).

[36] P. H. Lau, K. Takei, C. Wang, Y. Ju, J. Kim, Z. Yu, T. Takahashi, G. Cho, and A. Javey, *Nano Letters* **13**, 3864 (2013), <http://dx.doi.org/10.1021/nl401934a>.

[37] K. S. Kim, S. Karthikeyan, and N. J. Singh, *Journal of Chemical Theory and Computation* **7**, 3471 (2011), <http://dx.doi.org/10.1021/ct200586g>.

[38] M. K. Leong, V. S. Mastryukov, and J. E. Boggs, *The Journal of Physical Chemistry* **98**, 6961 (1994), <http://dx.doi.org/10.1021/j100079a013>.

[39] B. L. Kormos, C. J. Cramer, and W. L. Gladfelter, *The Journal of Physical Chemistry A* **110**, 494 (2006), <http://dx.doi.org/10.1021/jp051885+>.

[40] M. J. Frisch, G. W. Trucks, H. B. Schlegel, G. E. Scuseria, M. A. Robb, J. R. Cheeseman, G. Scalmani, V. Barone, B. Mennucci, G. A. Petersson, H. Nakatsuji, M. Cariati, X. Li, H. P. Hratchian, A. F. Izmaylov, J. Bloino, G. Zheng, J. L. Sonnenberg, M. Hada, M. Ehara, K. Toyota, R. Fukuda, J. Hasegawa, M. Ishida, T. Nakajima, Y. Honda, O. Kitao, H. Nakai, T. Vreven, J. A. Montgomery, Jr., J. E. Peralta, F. Ogliaro, M. Bearpark, J. J. Heyd, E. Brothers, K. N. Kudin, V. N. Staroverov, R. Kobayashi, J. Normand, K. Raghavachari, A. Renndell, J. C. Burant, S. S. Iyengar, J. Tomasi, M. Cossi, N. Rega, J. M. Millam, M. Klene, J. E. Knox, J. B. Cross, V. Bakken, C. Adamo, J. Jaramillo, R. Gomperts, R. E. Stratmann, O. Yazyev, A. J. Austin, R. Cammi, C. Pomelli, J. W. Ochterski, R. L. Martin, K. Morokuma, V. G. Zakrzewski, G. A. Voth, P. Salvador, J. J. Dannenberg, S. Dapprich, A. D. Daniels, . Farkas, J. B. Foresman, J. V. Ortiz, J. Cioslowski, and D. J. Fox, “Gaussian 09 revision d.01,” Gaussian Inc. Wallingford CT 2009.

[41] M. Burkatzki, C. Filippi, and M. Dolg, *The Journal of Chemical Physics* **126**, 234105 (2007).

[42] R. Jastrow, *Phys. Rev.* **98**, 1479 (1955).

[43] N. D. Drummond, M. D. Towler, and R. J. Needs, *Phys. Rev. B* **70**, 235119 (2004).

[44] C. J. Umrigar and C. Filippi, *Phys. Rev. Lett.* **94**, 150201 (2005).

[45] N. D. Drummond and R. J. Needs, *Phys. Rev. B* **72**, 085124 (2005).

[46] T. Kato, *Communications on Pure and Applied Mathematics* **10**, 151 (1957).

[47] C. J. Umrigar, M. P. Nightingale, and K. J. Runge, *The Journal of Chemical Physics* **99**, 2865 (1993).

[48] M. Casula, *Phys. Rev. B* **74**, 161102 (2006).

[49] L. Mitáš, E. L. Shirley, and D. M. Ceperley, *The Journal of Chemical Physics* **95**, 3467 (1991).

[50] P. J. Reynolds, D. M. Ceperley, B. J. Alder, and W. A. Lester, *The Journal of Chemical Physics* **77**, 5593 (1982).

[51] S. Grimme, *Journal of Computational Chemistry* **27**, 1787 (2006).

[52] S. Grimme, J. Antony, S. Ehrlich, and H. Krieg, *The Journal of Chemical Physics* **132**, 154104 (2010).

[53] Y. Zhao and D. Truhlar, *Theoretical Chemistry Accounts* **120**, 215 (2008).

[54] S. H. Vosko, L. Wilk, and M. Nusair, *Canadian Journal of Physics* **58**, 1200 (1980), <http://dx.doi.org/10.1139/p80-159>.

[55] J. P. Perdew, K. Burke, and M. Ernzerhof, *Phys. Rev. Lett.* **77**, 3865 (1996).

[56] C. Lee, W. Yang, and R. G. Parr, *Phys. Rev. B* **37**, 785 (1988).

[57] A. D. Becke, *The Journal of Chemical Physics* **98**, 5648 (1993).

[58] P. J. Stephens, F. J. Devlin, C. F. Chabalowski, and M. J. Frisch, *The Journal of Physical Chemistry* **98**, 11623 (1994), <http://dx.doi.org/10.1021/j100096a001>.

[59] D. G. Truhlar, *Chemical Physics Letters* **294**, 45 (1998).

[60] M. O. Sinnokrot and C. D. Sherrill, *The Journal of Physical Chemistry A* **108**, 10200 (2004), <http://dx.doi.org/10.1021/jp0469517>.

[61] S. Boys and F. Bernardi, *Molecular Physics* **19**, 553 (1970), <http://dx.doi.org/10.1080/00268977000101561>.

[62] F. B. van Duijneveldt, J. G. C. M. van Duijneveldt-van de Rijdt, and J. H. van Lenthe, *Chemical Reviews* **94**, 1873 (1994), <http://dx.doi.org/10.1021/cr00031a007>.

[63] S. Simon, M. Duran, and J. J. Dannenberg, *The Journal of Chemical Physics* **105**, 11024 (1996).

[64] M. Hasegawa and K. Nishidate, *Phys. Rev. B* **70**, 205431 (2004).

[65] A. Tkatchenko and O. A. von Lilienfeld, *Phys. Rev. B* **78**, 045116 (2008).

[66] K. E. Riley, J. A. Platts, J. Řezáč, P. Hobza, and J. G. Hill, *The Journal of Physical Chemistry A* **116**, 4159 (2012), pMID: 22475190, <http://dx.doi.org/10.1021/jp211997b>.

[67] N. N. Greenwood and A. Earnshaw, *Chemistry of the Elements (Second Edition)* (Butterworth-Heinemann, 1997).

[68] A. J. Misquitta, R. Maezono, N. D. Drummond, A. J. Stone, and R. J. Needs, *Phys. Rev. B* **89**, 045140 (2014).

[69] E. Lifshitz, *Soviet Phys. JETP* **2**, 73 (1956).

[70] V. Parsegian and B. Ninham, *Nature* **224**, 1197 (1969).

[71] T. Masuda, Y. Matsuki, and T. Shimoda, *Journal of Colloid and Interface Science* **340**, 298 (2009).

[72] J. Řezáč and P. Hobza, *Journal of Chemical Theory and Computation* **9**, 2151 (2013), <http://dx.doi.org/10.1021/ct400057w>.

- [73] J. Šponer, P. Jurečka, I. Marchan, F. J. Luque, M. Orozco, and P. Hobza, Chemistry – A European Journal **12**, 2854 (2006).
- [74] K. Hongo and R. Maezono, International Journal of Quantum Chemistry **112**, 1243 (2012).
- [75] J. Kolorenč, S. Hu, and L. Mitas, Phys. Rev. B **82**, 115108 (2010).
- [76] M. C. Per, K. A. Walker, and S. P. Russo, Journal of Chemical Theory and Computation **8**, 2255 (2012), <http://dx.doi.org/10.1021/ct200828s>.

SUPPORTING INFORMATION

Binding curve

For most of practical cases, we cannot expect the molecular dimer system to be accommodated within the possible size to be described by accurate basis sets, such as 'triple- ζ '(TZ) cc-pVTZ. In the present case actually, 'double- ζ '(DZ), cc-pVDZ, is the upper limit of the size even on the memory capacity of commercial supercomputers. For such a case, several schemes to correct biases due to less accurate basis sets are available. Schemes for basis set superposition error (BSSE) [1] corrects the 'unbalanced' accuracies to describe monomers and dimers, when they are used together to get binding energies. For an implementation of BSSE, we used here the counterpoise method. [2, 3] Schemes of the complete basis set (CBS) [4] were used to estimate an extrapolation to an enough large basis set.

Except for CCSD(T), we applied a CBS scheme by Truhlar [4] to get the corrected binding energy, ΔE_{CBS} , by the weighting as,

$$\Delta E_{\text{CBS}} = \frac{3^\gamma}{3^\gamma - 2^\gamma} \Delta E_3 - \frac{2^\gamma}{3^\gamma - 2^\gamma} \Delta E_2, \quad (\text{S-1})$$

where $\Delta E_{2,3}$ denote the energies evaluated by different basis set levels. For more reliability, we examined two different pairs for the correction, 'CBS': [(2,3) = (cc-pVDZ(DZ),cc-pVTZ(TZ))], and 'aCBS': [(2,3) = (aug-cc-pVDZ(aDZ),aug-cc-pVTZ(aTZ))]. The exponent, γ , is chosen as 3.4 (2.2) for HF and B3LYP-GD3 (MP2) as proposed by Truhlar *et al.*, [4] which is reported to be working well for non-covalent systems. [5]

For CCSD(T), the calculation was too costly to be done with larger basis sets other than cc-pVDZ level, making Truhlar's scheme not applicable to this case. Instead, we hence employed Sherrill's scheme [6],

$$\Delta E_{\text{CBS}}^{\text{CCSD(T)}} \approx \Delta E_{\text{CBS}}^{\text{MP2}} + \left(\Delta E^{\text{CCSD(T)}} - \Delta E^{\text{MP2}} \right)_{\text{cc-pVDZ}}, \quad (\text{S-2})$$

in which the extrapolation can be estimated only within a basis set, but assisted by further MP2 evaluations.

Comparisons of binding curves with/without corrections are summarized in Figs. S-2, S-3 and S-4 for SCF

(HF and DFT in the following context), MP2, and CCSD(T), respectively. In each figure, panel (a) represents the final results, while (b)-(d) show separated contributions to (a): In panels (b), the amount of BSSE corrections is found to increase as binding lengths gets shorter, because of the more overlapping, as expected. We see the more accurate basis sets used, the smaller the amount of the BSSE correction. Comparing panels (a) among the methods, we can see that correlated methods such as MP2 and CCSD(T) gives almost twice larger BSSE corrections than SCF methods. Comparison between panel (c) and (d) within each figure, we see that the dependence on basis sets gets weakened when BSSE corrections are applied. For SCF (Fig. S-2), the dependence seems almost completely disappeared, while for MP2 (Fig. S-3) there still remains the dependence especially on the predictions of the binding length. In SCF methods, the energy approaches to the CBS limit always from bottom, while in MP2 it is alternating, namely the energy by DZ/TZ is above the limit but below by more improved basis set, aDZ/aTZ. In Fig. S-2 (a), we can also confirm that the BFD-VTZ result is quite close to the CBS limit, supporting a confidence about the present DMC using this basis set.

The larger BSSE corrections for correlated methods (MP2 and CCSD(T)) than those for SCF. This can be explained as follows: Since the correction should be zero in the CBS limit, the amount of the correction would be a measure how far the basis set adopted is from CBS limit in the sense of the accuracy in each method. Suppose a basis set being sufficient to describe occupied orbitals used in SCF, but it is not the case also for further unoccupied orbitals in general, which are used in correlated methods such as CCSD(T) or MP2. The BSSE corrections with the same basis set is then getting larger for correlated methods than for SCF.

Nodal surface dependence and time-step errors

For the present DMC results, we have to examine the biases due to the approximations we applied, namely, the time-step approximation [7] and the fixed-node approximation. [8] In the sense of finite discretization of propagations, the smaller time-step, δt , would be reliable, but too small step cannot achieve such a random walk covering over the sampling space within a limited number of steps by a tractable computation. Fig. S-5 shows the time-step (δt) dependence of the DMC binding curves, evaluated for Type-A using B3LYP nodal surfaces. The curves seem to be converging within errorbars, justifying the present choice of $\delta t = 0.02$ with enough high acceptance ratio being more than 99.5%.

The dependence of the binding curve (Type-A/ $\delta t = 0.02$) on the nodal surfaces is shown in Fig. S-5 (b) in absolute energy values, from which we can identify which

nodal surface gives the variationally best estimation.[8] We noted that T -move scheme [9] is used in the present study to preserve the variational principle even under the locality approximation [10] for pseudo potentials. The choice of the nodal surfaces hardly changes the global shape such as the binding length. We also see that B3LYP nodes gives the variationally best description. Though there is still not enough convincing explanations, B3LYP nodes for DMC are also reported as the best for several other systems. [11–14]

* kenta.hongo@mac.com

- [1] van Duijneveldt, F. B.; van Duijneveldt-van de Rijdt, J. G. C. M.; van Lenthe, J. H. State of the Art in Counterpoise Theory. *Chemical Reviews* **1994**, *94*, 1873–1885.
- [2] Boys, S.; Bernardi, F. The calculation of small molecular interactions by the differences of separate total energies. Some procedures with reduced errors. *Molecular Physics* **1970**, *19*, 553–566.
- [3] Simon, S.; Duran, M.; Dannenberg, J. J. How does basis set superposition error change the potential surfaces for hydrogen-bonded dimers? *The Journal of Chemical Physics* **1996**, *105*, 11024–11031.
- [4] Truhlar, D. G. Basis-set extrapolation. *Chemical Physics Letters* **1998**, *294*, 45–48.
- [5] Šponer, J.; Jurečka, P.; Marchan, I.; Luque, F. J.; Orozco, M.; Hobza, P. Nature of Base Stacking: Reference Quantum-Chemical Stacking Energies in Ten Unique B-DNA Base-Pair Steps. *Chemistry – A European Journal* **2006**, *12*, 2854–2865.
- [6] Sinnokrot, M. O.; Sherrill, C. D. Highly Accurate Coupled Cluster Potential Energy Curves for the Benzene Dimer: Sandwich, T-Shaped, and Parallel-Displaced Configurations. *The Journal of Physical Chemistry A* **2004**, *108*, 10200–10207.
- [7] Umrigar, C. J.; Nightingale, M. P.; Runge, K. J. A diffusion Monte Carlo algorithm with very small time??step errors. *The Journal of Chemical Physics* **1993**, *99*, 2865–2890.
- [8] Reynolds, P. J.; Ceperley, D. M.; Alder, B. J.; Lester, W. A. Fixed-node quantum Monte Carlo for molecules. *The Journal of Chemical Physics* **1982**, *77*, 5593–5603.
- [9] Casula, M. Beyond the locality approximation in the standard diffusion Monte Carlo method. *Phys. Rev. B* **2006**, *74*, 161102.
- [10] Mitáš, L.; Shirley, E. L.; Ceperley, D. M. Nonlocal pseudopotentials and diffusion Monte Carlo. *The Journal of Chemical Physics* **1991**, *95*, 3467–3475.
- [11] Hongo, K.; Cuong, N. T.; Maezono, R. The Importance of Electron Correlation on Stacking Interaction of Adenine-Thymine Base-Pair Step in B-DNA: A Quantum Monte Carlo Study. *Journal of Chemical Theory and Computation* **2013**, *9*, 1081–1086.
- [12] Hongo, K.; Maezono, R. A benchmark quantum Monte Carlo study of the ground state chromium dimer. *International Journal of Quantum Chemistry* **2012**, *112*, 1243–1255.
- [13] Kolorenč, J.; Hu, S.; Mitas, L. Wave functions for quantum Monte Carlo calculations in solids: Orbitals from density functional theory with hybrid exchange-correlation functionals. *Phys. Rev. B* **2010**, *82*, 115108.
- [14] Per, M. C.; Walker, K. A.; Russo, S. P. How Important is Orbital Choice in Single-Determinant Diffusion Quantum Monte Carlo Calculations? *Journal of Chemical Theory and Computation* **2012**, *8*, 2255–2259.

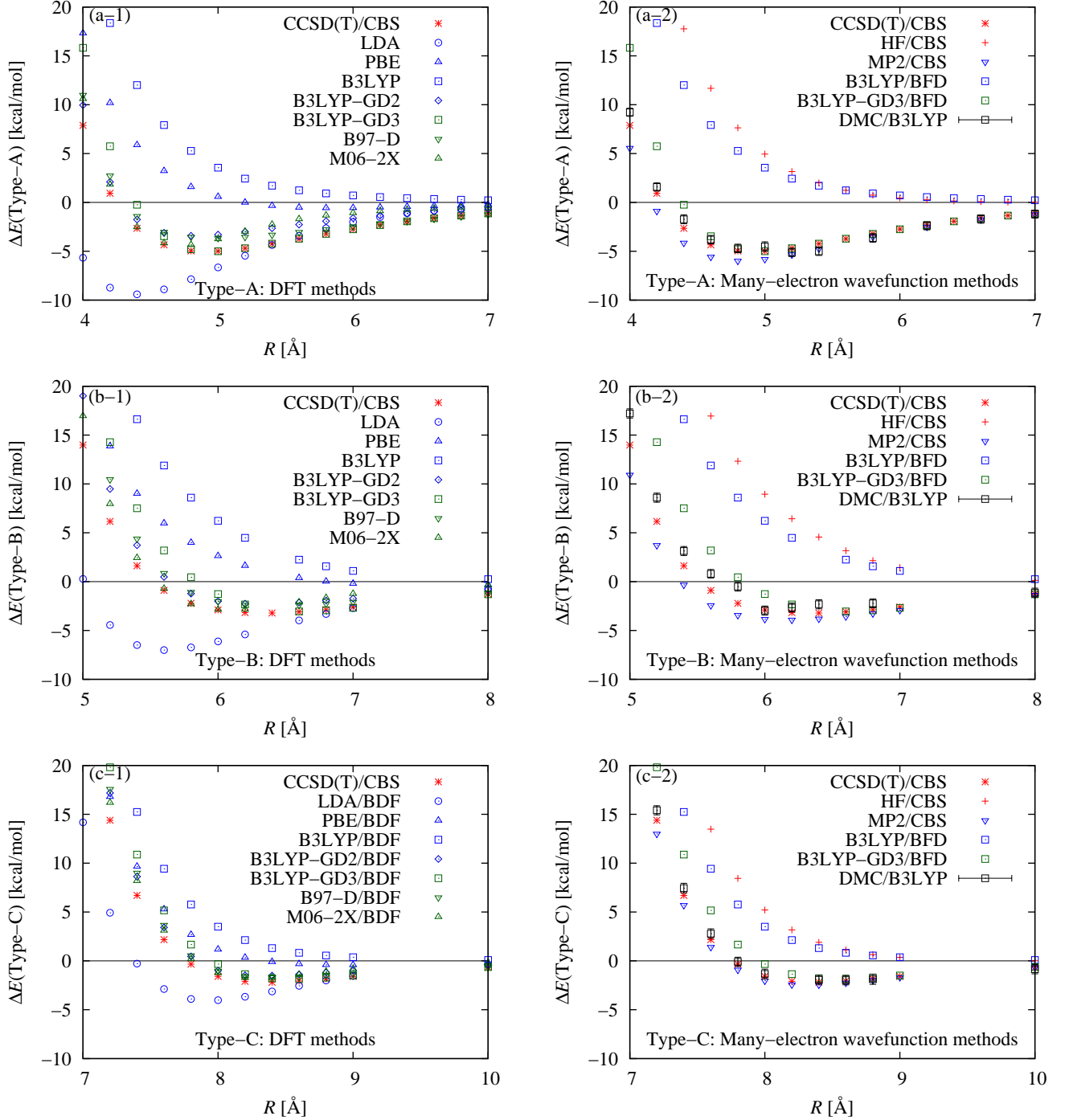


FIG. S-1. Binding curves for Type-A [panels (a)], Type-B [panels (b)], and Type-C [panels (c)], evaluated by several DFT [panel (a/b/c-1)] and correlated methods [panel (a/b/c-2)]. Results are corrected by CBS scheme if applicable. DMC results are evaluated using B3LYP/BDF-VTZ fixed nodes.

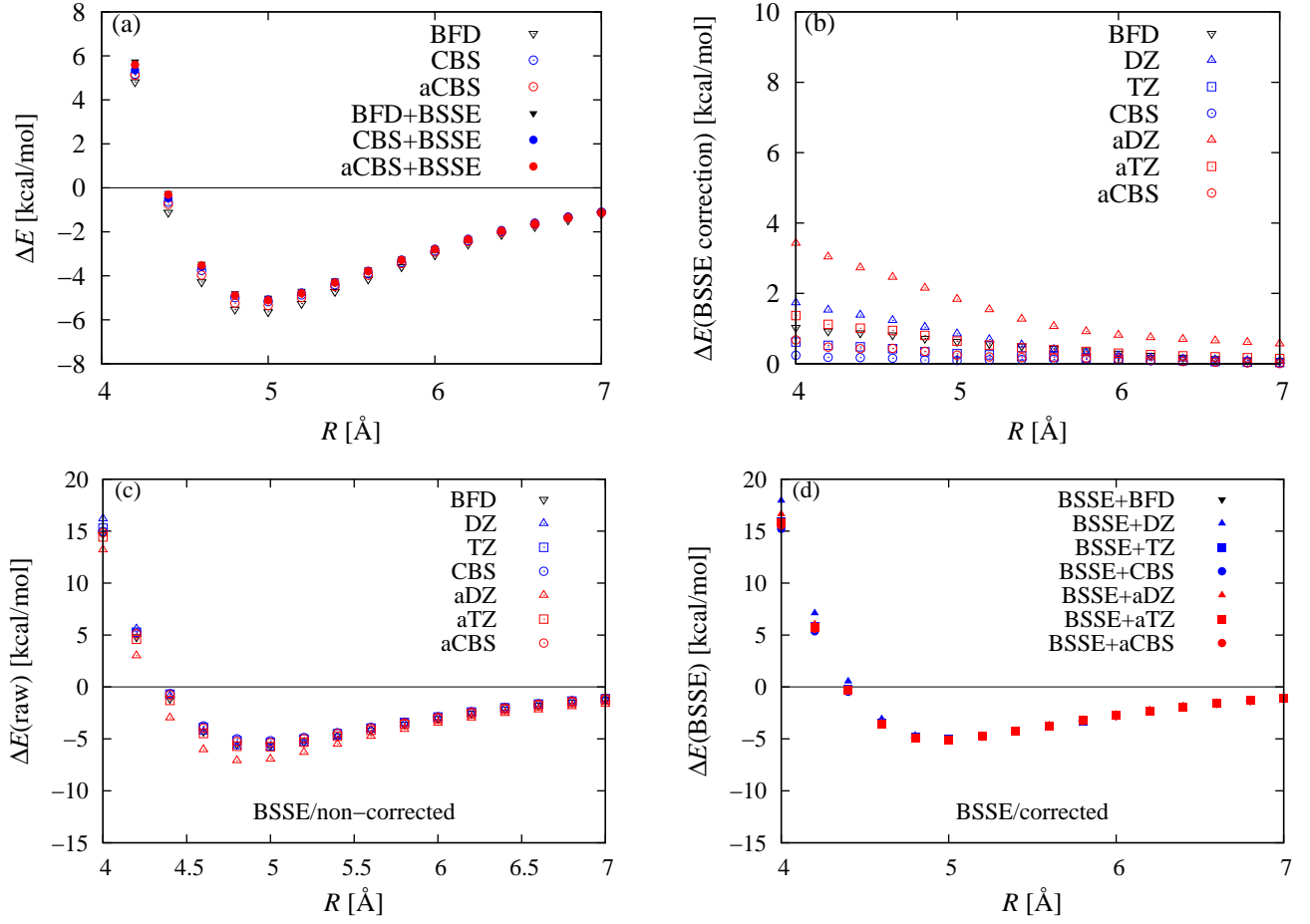


FIG. S-2. Binding curves and corrections for Type-A by B3LYP-GD3. Panel (a) shows the final binding curves after possible corrections, while (b)-(d) are separated contributions and comparisons with/without BSSE corrections. CBS (aCBS) stands for the CBS limit estimated by DZ/TZ (aDZ/aTZ) basis sets.

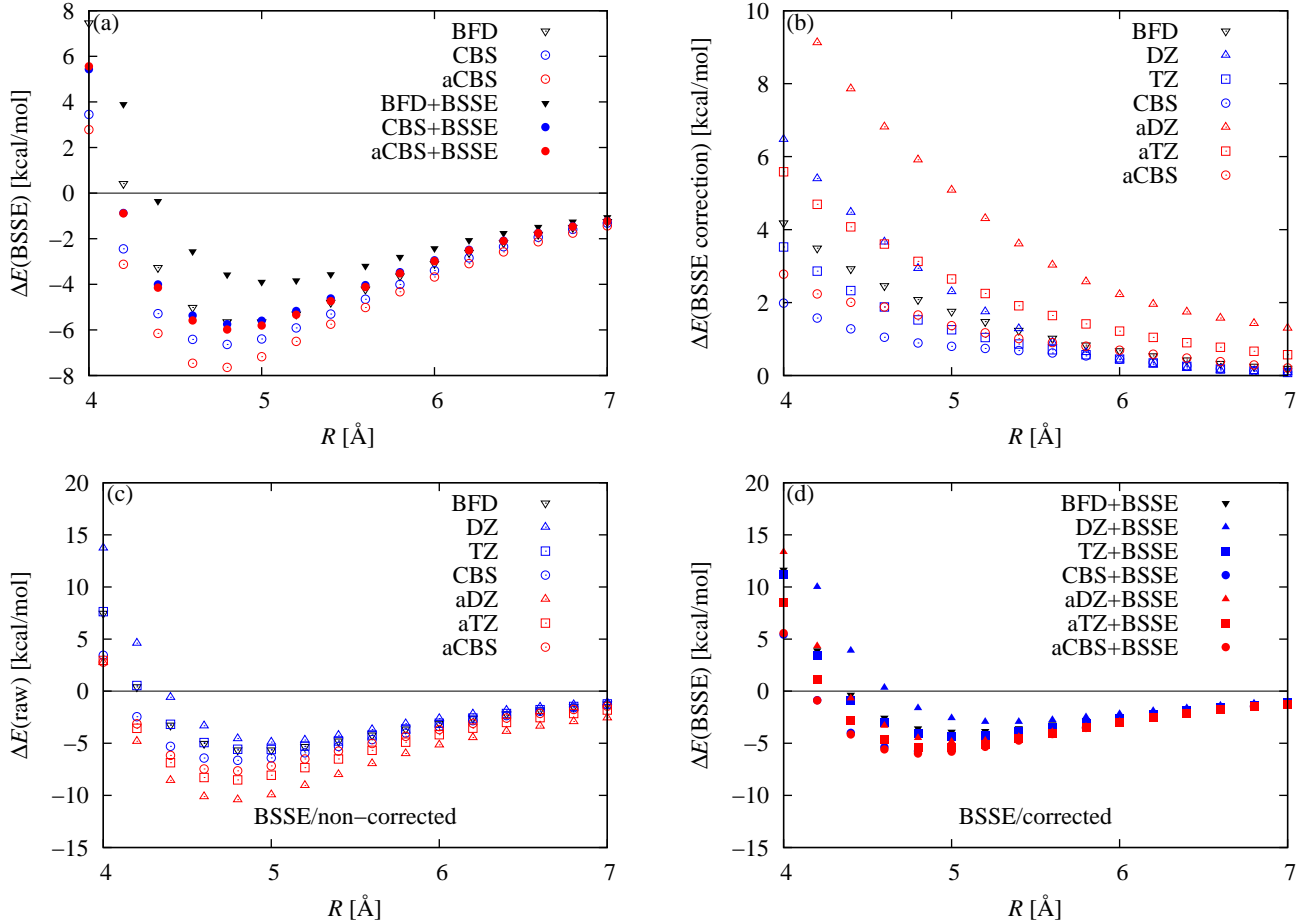


FIG. S-3. Binding curves and corrections for Type-A by MP2. Panel (a) shows the final binding curves after possible corrections, while (b)-(d) are separated contributions and comparisons with/without BSSE corrections. CBS (aCBS) stands for the CBS limit estimated by DZ/TZ (aDZ/aTZ) basis sets.

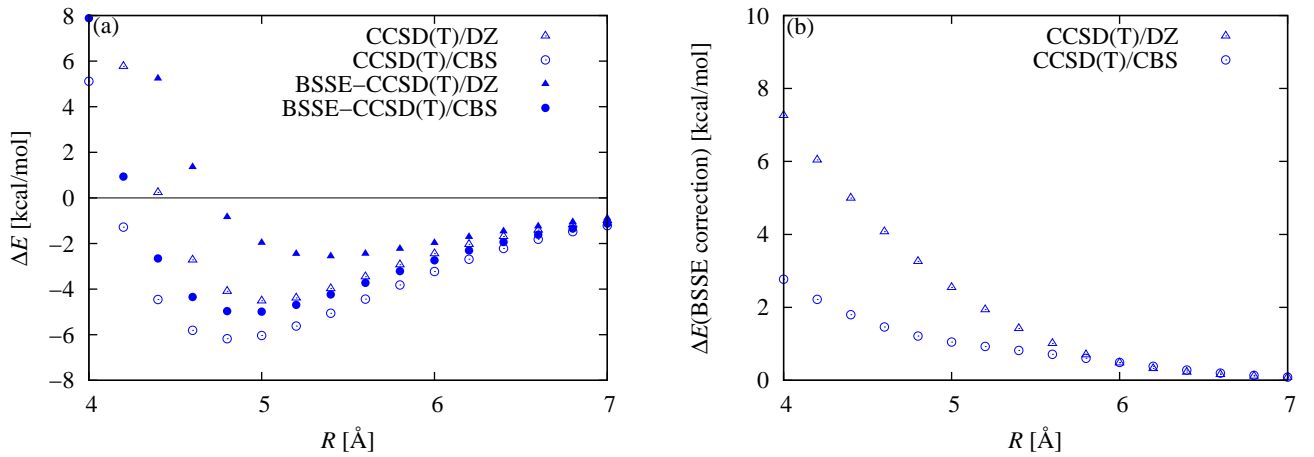


FIG. S-4. Binding curves and corrections for Type-A by CCSD(T). Panel (a) shows the final binding curves after possible corrections, while (b) shows the amount of BSSE contributions. 'CCSD(T)/DZ[CBS]' stands for the raw value without any corrections by DZ basis sets [CBS limit], while 'BSSE-CCSD(T)/DZ[CBS]' means that with BSSE corrections.

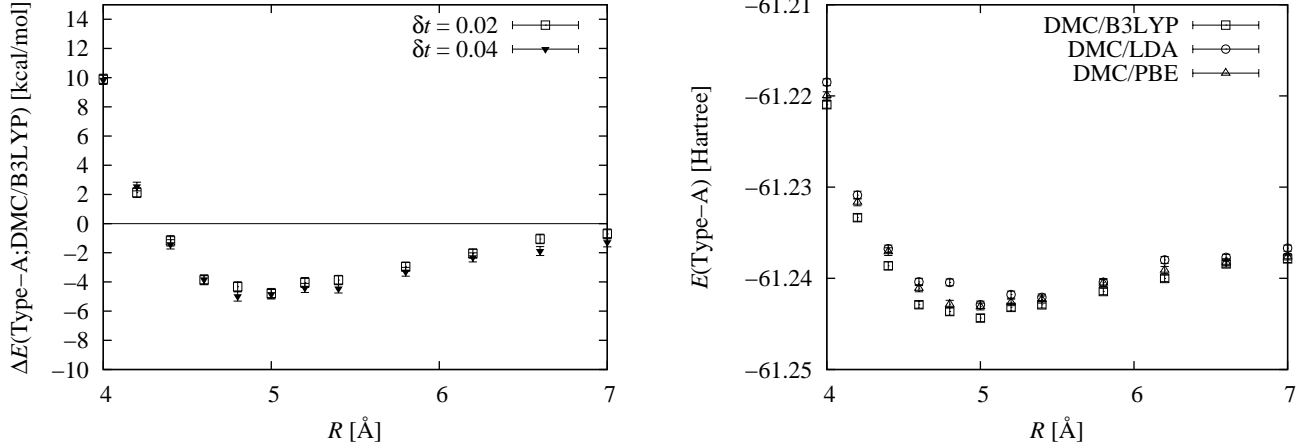


FIG. S-5. Time step dependence (left panel) and the nodal surface dependence (right panel) of the DMC binding curve for Type-A. For the left panel, DMC/B3LYP results are shown, which is variationally best in the right panel.